Purcell enhanced and indistinguishable single-photon generation from quantum dots coupled to on-chip integrated ring resonators

Łukasz Dusanowski,[*,†] Dominik Köck,[†] Eunso Shin,[‡] Soon-Hong Kwon,[‡] Christian Schneider,[†,¶] and Sven Höfling[†,§]

†*Technische Physik and Würzburg-Dresden Cluster of Excellence ct.qmat, University of Würzburg, Physikalisches Institut and Wilhelm-Conrad-Röntgen-Research Center for Complex Material Systems, Am Hubland, D-97074 Würzburg, Germany*

‡*Department of Physics, Chung-Ang University, 156-756 Seoul, Korea*

¶*Institute of Physics, University of Oldenburg, D-26129 Oldenburg, Germany*

§*SUPA, School of Physics and Astronomy, University of St Andrews, KY16 9SS St Andrews, UK*

E-mail: lukasz.dusanowski@uni-wuerzburg.de

Abstract

Integrated photonic circuits provide a versatile toolbox of functionalities for advanced quantum optics applications. Here, we demonstrate an essential component of such a system in the form of a Purcell enhanced single-photon source based on a quantum dot coupled to a robust on-chip integrated resonator. For that, we develop GaAs monolithic ring cavities based on distributed Bragg reflector ridge waveguides. Under resonant excitation conditions, we observe an over twofold spontaneous emission rate enhancement using Purcell effect and gain a full coherent optical control of a QD-two-level system via Rabi oscillations. Furthermore, we demonstrate an on-demand

single-photon generation with strongly suppressed multi-photon emission probability as low as 1% and two-photon interference with visibility up to 95%. This integrated single-photon source can be readily scaled up, promising a realistic pathway for scalable on-chip linear optical quantum simulation, quantum computation and quantum networks.

Keywords

quantum dot, single-photon source, integrated photonics, ring resonator, Purcell, two-photon interference

Advanced quantum optics applications such as quantum networks, quantum simulation and quantum computing require single-photon sources with simultaneously high efficiency and degree of photons indistinguishability. Among different kinds of emitters self-assembled quantum dots (QDs) coupled to optical cavities have been shown to be one of the brightest on-demand single-photon sources up to date (SPS),[1–3] which can simultaneously reach almost unity single-photon indistinguishability and purity as well extraction efficiency as high as 60%.[3–6] Those advances allowed already for demonstration of on-demand CNOT-gates,[7–9] heralded entanglement between distant spin qubits,[10,11] quantum teleportation[12,13] or the recent realization of 20-photon boson sampling.[14] This tremendous progress in QD-based single-photon sources have been achieved by a combination of resonant excitation[3,15,16] to eliminate emission time jitter and cavity quantum electrodynamics to overcome fundamental limitations set by intrinsic exciton-phonon scattering inherent in solid-state platform.[17]

As the quantum optics experiments have increased in complexity, there has been an increasing need to transition bulk optics experiments to integrated photonic platforms, where all components could be placed on the same chip. It means that single photons sources, photonic circuitry and detectors could be optically interconnected with very small losses and allow to control single-photon states with greater fidelity. More-importantly integrated circuits combined with quantum emitters are believed to be a reliable approach to achieve

full scalability towards large scale quantum optics.[2,18,19]

The GaAs material system with embedded QDs seems to be a perfectly suited system for that purpose, where both fully homogeneous[20–24] and heterogeneous[25–28] integrated photonic circuits were realized. In this approach, light can be directly coupled into in-plane waveguides (WGs) and combined with other functionalities on a chip such as phase shifters,[29,30] beam splitters,[20,27,31] filters,[26,32,33] detectors[24,34] and other devices for light propagation, manipulation and detection on a single photon level. Moreover, integrated circuits allow to spatially separate excitation and detection spots, which straightforwardly enables applying resonant driving schemes to slow-down decoherence processes and reduce on-demand emission time-jitter.[35–40]

Among different on-chip QD-integration implementations, a particular emphasis over last years has been devoted to photonic crystal (PhC) and nanobeam WGs.[21,23,41,42] Especially, pulsed resonance fluorescence generation of indistinguishable single photons in waveguides was achieved recently.[38,39] Despite this progress, the persistent problem of PhC and nanobeam WGs systems are their large propagation losses and fragility,[19] limiting dimensions of freestanding circuits to a few hundred microns. Combination of PhC and nanobeam WGs with GaAs ridge waveguides[43] or heterogeneous integration with SiO_2/Si_3N_4 ridge waveguides[25–27] have been also proposed, however, it demands complicated multi-step fabrication process and introduces losses at interfaces. Alternative approach offering more robust design with high mechanical stability are monolithic ridge waveguides. Typically, those are based on GaAs core layer and distributed Bragg reflector (DBR) or AlGaAs layers cladding. Using this system, complex integrated circuits with large footprints have been realized[20,30,44] promising a clear path towards scalability. Using GaAs ridge waveguides full on-chip second-order correlation experiments have been implemented[44] and pulsed resonance fluorescence demonstrated,[37,40,45] which allowed recently for single-photon generation with non-corrected two-photon interference visibility of 97.5%.[40] The main challenge in the broader application of GaAs ridge waveguides with QDs in quantum integrated photonics is relatively low cou-

pling efficiency of photons emitted from QD to waveguide mode (15-22% into each WG arm), due to the low-refractive-index contrast between GaAs and AlGaAs materials. One route to overcome this problem is the application of the Purcell effect to boost up QD emission funnelling into the WG mode.[46]

Hereby we will combine cavities with ridge waveguides and show that such a system has the potential of achieving simultaneously high coupling efficiency and near-unity single-photon indistinguishability in reliable integrated circuit platform. Among different types of cavities, ring resonators are well established on-chip functionalities in integrated circuits.[47] They are commonly used as filters,[25,26,32] switches[48] or parametric down-conversion pair sources.[49] Due to easily achievable high-quality factors (Q), they are also perfectly suited for increasing light-matter interaction with quantum emitters.[25,50] Recently, devices combining the InAs QDs with ring resonators have been realized by the heterogeneous integration of GaAs and Si_3N_4 platforms. Spontaneous emission enhancement factors up to 4 have been observed,[25] however, experiments have been limited to non-resonant continuous-wave (cw) excitation only, which is known to degrade the purity and indistinguishability of emitted photons, so that high-performance on-demand SPS ring devices were not realized yet.

In this article, we demonstrate resonantly driven triggered SPSs consisting of self-assembled InAs/GaAs QDs coupled to on-chip ring resonators based on the DBR ridge waveguides within the same GaAs wafer. By spectral tuning of the QD emission into the ring cavity mode, we achieve an over twofold spontaneous emission rate enhancement, reveled by time-resolved studies. Furthermore, we observe Rabi oscillations visible from the QD emission intensity variation as a function of pump pulse area, demonstrating coherent optical control. Finally, we show a generation of single and indistinguishable photons on demand by performing second-order correlation experiments in Hanbury-Brown-Twiss (HBT) and Hong-Ou-Mandel (HOM) configurations. By employing resonant excitation scheme within on-chip ring-bus-waveguide system we observe strongly suppressed multi-photon emission probability better than 1% and two-photon interference with visibility up to 95%. Combina-

tion of those results makes our DBR ridge ring resonator single-photon source a competitive with other integrated structures approaches.

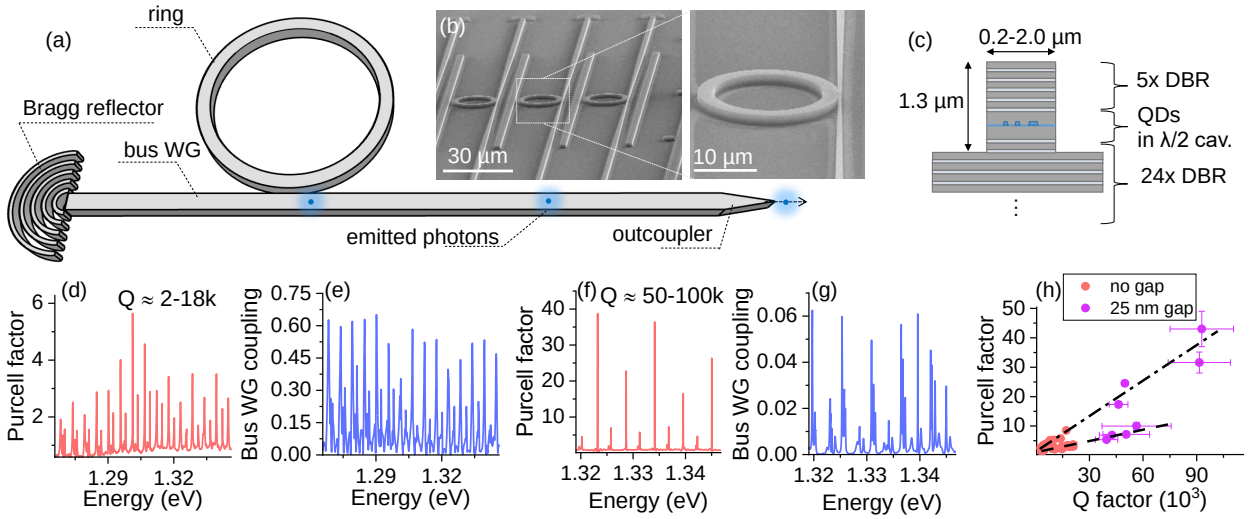

Figure 1: On-chip integrated ring resonator device. (a) Artistic scheme of the DBR waveguide (WG) based ring resonator. Single quantum dots are placed within the core of the WG and excited optically from the top. Emitted photons are collected from the side facet of the structure within the tapered out-coupler. (b) Scanning electron microscope images of the fabricated ring resonator devices with radius R of 10 μm. (c) DBR WG cross-section with marked layers. (d),(f) Simulated Purcell factor vs energy for the 2 μm width ring resonator with an outer radius of 10 μm coupled to 0.2 μm width bus WG and 0 and 25 nm ring-bus-WG gap, respectively. (e),(g) Simulated QD emission coupling efficiency into the bus WG for 0 and 25 nm gap structures, respectively. Very high quality factor Q of the 25 nm gap ring cavity required limiting the simulation spectral window to 20 nm. (h) Purcell factor vs Q factor taken from Fig. 1(d) and (f), reveling clear linear dependence for fundamental (dot-dashed line) and higher-order radial modes (dashed line).

An artistic sketch of our integrated system is shown in Fig.1(a). It consists of following elements: the ring resonator coupled in-plane to bus waveguide, circular Bragg grating on the one end of the WG working as a reflector and tapered out-coupler designed to minimize reflection and optimize out-coupling efficiency into the off-chip collection optics (more details in Supporting Information). To operate our device as an on-chip SPS, the QD is excited from the top of a ring and the single-photon emission is collected from the bus waveguide after more than 1 mm travel distance by the tapered out-coupler localized on the sample edge. The cross-section of the DBR WG is shown in Fig.1(c).

In this work, we consider two ring resonator designs: (i) based on uniform single-mode

(SM) WG width of 0.8 μm of both the ring and the bus section and (ii) based on multi-mode (MM) 2.0 μm width WG uniform within the ring and tapered bus WG narrowing from 2.0 μm to single-mode 0.2 μm width section close to the coupling region. A tapering section in case of second design ensures that light is coupled and guided only in the fundamental transverse-electric (TE) mode of the MM bus waveguide, which can be latter efficiently back coupled to single-mode WG using mode converters (more details in Supplementary Information). The first design is simpler and more straightforward to combine with other on-chip SM functionalities, such as beam-splitters or interferometers. However, small width WGs tends to have larger propagation losses, since less tightly confined mode is more susceptible to scattering due to sidewalls roughness.[51] Indeed, in case of the considered system, we observe propagation losses on the level of 2-3.5 dB/mm for 2.0 μm width WGs and 4-7 dB/mm in case of 0.8 μm WGs.

To optimize the structure geometry for maximized Purcell, we fabricated a set of ring devices with various diameter and ring-bus-WG spacing (gap), and performed a systematic check of the Q-factors via optical measurements. For rings with $R \leq 5$ μm the quality factor was limited to 1-2k due to the fabrication imperfections (mainly surface roughness). In contrary, for rings with $R \geq 10$ μm modes with Q exceeding 7-12k were observed. Within such mode volume to Q factor trade-off, we concluded that rings with $R = 10$ μm are the most promising in terms of obtainable Purcell (more details in Supplementary Information).

For the quantitative estimate of the maximal obtainable Purcell enhancement and waveguide coupling efficiency, we simulated photonic properties of our devices using Finite Difference Time Domain (FDTD) method. By placing a point dipole in the ring cavity mode, we calculated Purcell enhancement factor, defined as power emitted by a dipole source in the ring normalized to the power emitted by the dipole in a homogeneous (bulk) environment. Results of simulations for a ring with WG profile of 2.0 x 1.3 μm, 10 μm outer radius and 0.2 μm bus WG are presented in Figures 1(d) and (f) for gap-less and 25 nm gap structures, respectively. Clear sharp peaks at energies fulfilling traveling wave resonance conditions

$\lambda m = 2\pi n_g R$ for fundamental and higher-order radial modes can be distinguished, where m is a mode number, λ is a wavelength, n_g is a group refractive index and R is a ring radius. The simulated Purcell factors can reach values up to 6 with Q of 2k-18k for gap-less rings and Purcell up to 40 with Q of 50-100k for 25 nm gap rings. In Fig.1(e) the efficiency of the QD emission coupling into the bus WG is plotted for gap-less ring device. Values as high as 67% are obtainable, which consist of 70% QD-to-ring and 96% ring-to-bus-WG coupling contributions. Despite very high Purcell for 25 nm gap rings and thus almost unity coupling into the ring cavity mode, a relatively low coupling of 2-6% into the bus WG is expected, as shown in Fig. 1(g). With successive increase of the gap to 50 nm, WG coupling decreases even further, while Purcell seems to be unaffected (see Supplementary Information). Taken together, these results suggest that maximal obtainable Purcell for 10 μm radius rings is 40 and it is limited by bending losses. By plotting the Purcell factor vs Q for each mode, linear dependencies for fundamental and higher-order radial modes are observed as shown in Fig. 1(h). Following this relation, Purcell of 5-6 for Q of 10k and 10-12 for Q of 20k is expected. Similar simulations for rings placed inside the bus WG (negative gap) are summarized in Supplementary Information. Interestingly, we found that for -100 nm gap, the total bus WG coupling efficiencies up to 90% seems to be feasible with a moderate Purcell of around 2.

For optical characterization of our ring devices, we use top-excitation and side-detection micro-photoluminescence setup and cooldown sample to 4.5 K using a high-stability closed-cycle cryostat. The PL signal is collected from side facet after around 1 mm travel distance in the bus WG. First, we consider MM ring resonator with 10 μm radius and 100 nm nominal gap between the ring and tapered bus WG. In Figure 1(b) scanning electron microscope (SEM) images of the example fabricated ring resonator are shown. Higher magnification SEM images suggest that the GaAs cavity layer is not completely etched (effectively gap is $<$100 nm). Figure 2(a) shows a side collected photoluminescence (PL) spectra from a QD_1 under above-band gap cw excitation. A single emission line at 1.337 eV is visible with the

setup resolution limited linewidth. The inset in Fig. 2(a) shows investigated ring modes with Q factor values of around 6-7k, probed by photoluminescence at high power (the ensemble of QDs act as a spectrally broad light source). We tune the QD emission energy across the ring cavity mode by increasing the sample temperature. At around 14 K a resonance of the QD emission with the ring mode is established, as shown in Fig. 2(b).

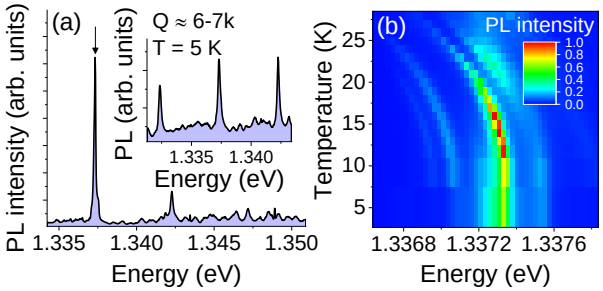

Figure 2: (a) Side detected photoluminescence spectrum from QD_1 recorded under non-resonant cw excitation and temperature of 5 K. Inset: Optical modes of the ring under investigation. (b) Temperature dependence of the QD_1 PL spectrum.

Next, device characteristics under s-shell resonant excitation were checked. Figure 3(a) shows side detected pulsed resonance fluorescence spectra from QD_1. In Inset of Fig. 3(a) the peak intensity versus the square root of the incident power is shown. Clear oscillatory behavior with damping at higher power is observed, which is clear evidence of Rabi oscillations related to coherent control of the QD two-level system. The data have been fitted with exponentially damped cosine function assuming phonon-related dephasing included in quadratic exponential damping term.[52]

To verify Purcell enhancement, we performed time-resolved resonance fluorescence measurements for different QD-cavity detunings as plotted in Fig. 3(b)-(c). All time traces exhibit mono-exponential decays. In strongly detuned case, beside QD-related emission decay, non-filtered laser contribution is also visible. At a temperature of 14 K, corresponding to the QD-cavity resonance, the shortest lifetime of 230 ps has been observed [time trace with blue points in Fig. 3(b)]. In case of 0.37 meV detuning [magenta points in Fig. 3(b)] time constant of 480 ps has been recorded. For comparison, in case of QDs coupled to

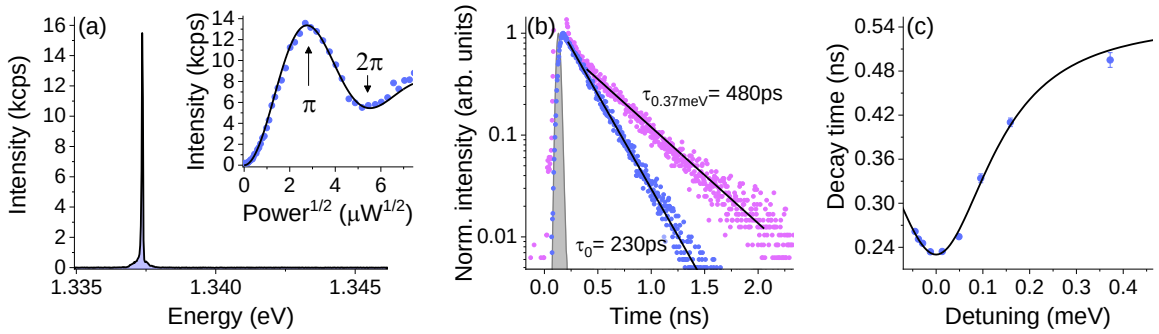

Figure 3: (a) Pulsed resonance fluorescence spectrum of QD_1 at 5 K. Inset: Resonance fluorescence intensity vs square root of power demonstrating Rabi oscillations. (b) Time-resolved resonance fluorescence traces recorded for 0.37 meV and no QD-cavity detuning. (c) Resonance fluorescence decay time vs QD-cavity energy detuning demonstrating Purcell enhancement.

straight ridge waveguides, we observe decay time constants on the level of 500-580 ps under resonant driving conditions.[40] By comparing 230 ps with the 500 ps lifetime, we can extract an over twofold radiative rate enhancement for the considered QD. The measured decay time as a function of detuning [Fig. 3(c)] is well fitted by the standard weak-coupling theoretical model (black curve) assuming coupling to the cavity mode with a quality factor of 7k, and considering that the emission rate into cavity follows a Lorentzian dependence with respect to the detuning. From fit, we extracted a maximum 2.4-fold enhancement of the spontaneous emission rate with Purcell factor F_p of 1.4 assuming that QD emission rate outside ring cavity mode is equal to emission rate in bulk GaAs (more details in Supporting Information). For the Purcell of 1.4, coupling efficiency into the cavity mode β, reaches values as high as 58% following formula $\beta = F_P/(F_P + 1)$, in respect to 30-44% coupling efficiency limitation in the non-structured WGs. Assuming 96% coupling between ring and bus WG, we expect an overall coupling efficiency of 55%. To cross-check this value, we additionally estimated the QD-bus-WG coupling efficiency, based on the single-photon detector counts and total efficiency of the circuit (more details in Supplementary Information). By careful calibration of the setup transmission, we obtained the total device extraction efficiency of 2.4% into the first detection lens and lower limit of QD-WG coupling on the level of 10%. We point out

that, QD-WG coupling efficiency was derived assuming that all on-chip functionalities such as reflector, tapers and out-coupler perform as good as theoretically expected, which most likely strongly underestimate the calculated efficiency value (more details in Supplementary Information).

To characterize our ring device single-photon emission statistics, auto-correlation experiments at a temperature of 5 K have been performed on the resonance fluorescence signal filtered out from a broader laser profile and phonon sidebands. In Fig. 4(a) a second-order correlation function histogram recorded in HBT configuration under π-pulse excitation is shown. At zero delay it shows clear antibunching with almost perfectly vanished multi-photon emission probability of $g^{(2)}(0) = 0.0191 \pm 0.007$. The experimental data is fitted by two-sided mono-exponential decay with a time constant of 260 ps, convoluted with the setup instrumental response function (IRF) with a width of 50 ps.

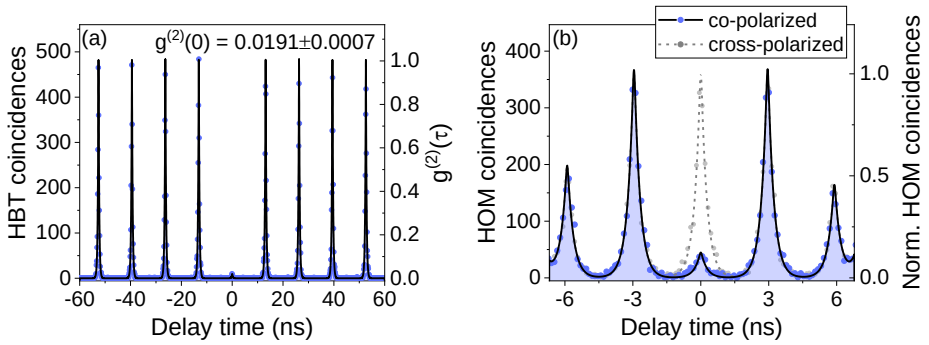

Figure 4: (a) Second order correlation function histogram recorded for pulsed resonance fluorescence under π-pulse excitation power. The value of $g^{(2)}(0)$ is calculated from the integrated photon counts in the zero-delay peak divided by the average of the adjacent set of peaks, while the uncertainty of the $g^{(2)}(0)$ is based on the standard deviation of the Poissonian peaks integrated counts. (b) Two-photon interference Hong-Ou-Mandel histogram recorded for 3 ns time separated co- (blue pints) and cross-polarized (grey points) single photons under pulsed resonance fluorescence and π-pulse excitation power.

Next, we test the indistinguishability of emitted photons through Hong-Ou-Mandel (HOM) interference experiments. For that purpose, we excite QD_1 by a pair of pulses separated by 3 ns. Two subsequently emitted photons are then filtered by a monochromator and introduced into fibre-based 3 ns delay unbalanced interferometer, where a delay between

them is compensated to superimpose single-photon pulses on the beam splitter.[1] A resulted two-photon interference histogram for orthogonal (gray points) and parallel (blue points) polarized photons is shown in Figure 4(b). The histogram consists of five 3 ns delayed peaks of the central cluster. In the case of identical polarizations, an almost vanishing zero-delay peak is observed. In contrast, for two photons with cross-polarization, the zero-delay peak has the same intensity as its adjacent ±3 ns delayed peaks. To evaluate the zero-delay peak area in respect to the neighbouring peaks the experimental data have been fitted with the two-side exponential decay functions convoluted with the setup IRF (more details in Supplementary Information). Upon the fitting procedure, we obtain a raw value of two-photon interference visibility of 0.90±0.02. After including the residual multi-photon probability of $g^{(2)}(0) = 0.0191$, as well as non-perfect interferometer visibility and splitting ratio[1] we determined a corrected degree of indistinguishability to be 0.95±0.02.

Similar optical characterization has been repeated on two other ring devices, with radius of 10 μm and 40 μm, respectively. In case of second 10 μm radius ring, the shortest lifetime of 210 ps was observed ($F_p = 1.7$) with $g^{(2)}(0)$ of 0.035±0.001 and corrected indistinguishability of 0.93±0.02. In case of 40 μm radius ring, no significant Purcell enhancement was observed (lifetime of 400 ps), while emitter indicated very good single-photon performance with $g^{(2)}(0)$ of 0.04±0.01 and corrected indistinguishability of 0.95±0.02 (corresponding graphs and more details in Supplementary Information).

Demonstration of high-performance SPSs coupled to on-chip resonators is an important step towards large scale implementations of quantum photonic circuits. Within the investigated GaAs platform, our QD-ring devices could be straightforwardly combined with integrated beam splitters,[20,30,53] which inherently offers near-perfect mode-overlap and very-high stability of the optical path-lengths, which enable high-fidelity quantum interference on-chip - an essential component for quantum information processing. Monolithic integration of QDs with GaAs circuits might be thus considered as a reliable pathway towards full on-chip scalability, both in terms of realizing mechanically stable large footprint circuit, as

well as in terms of fulfilling 1% two-photon gate operation error threshold and 67% total efficiency threshold required for fault-tolerant quantum computing.[54,55]

In this letter, we have demonstrated the on-demand single-photon source based on InAs QD coupled to on-chip ring resonator. By combining a robust DBR ridge WG platform with the ring cavity, we overcome an intrinsic limitation of the monolithic ridge WGs coupling efficiency by utilizing a Purcell effect. We observed an over two-fold spontaneous emission enhancement, proven by time-resolved resonance fluorescence studies. We demonstrated near-background free single-photon emission with $g^{(2)}(0) = 0.0191 \pm 0.0007$ and near-unity indistinguishability of 0.95±0.02. To best of our knowledge, it is the first demonstration of resonance fluorescence studies on the on-chip integrated ring resonators showing optical coherent control and on-demand indistinguishable single-photon generation. Taken the high degree of indistinguishability of the on-chip generated photons shown here, our structures could be used to realize various optical quantum-computing algorithms, interference of multiple photons, and the generation of photonic cluster states. We believe, that our devices could be further improved in terms of performance by the better spatial alignment of the ring cavity mode and QD position, to utilize larger Purcell enhancement and coupling efficiency, while keeping high single-photon indistinguishability. Moreover, our structures could be straightforwardly monolithically integrated with other on-chip functionalities including beam-splitters, phase shifter, detectors and other devices, suitable for handling large scale advanced quantum optics experiments on-chip. A potential of manufacturing such circuits, combined with the high purity and potentially a high efficiency indistinguishable single-photon sources, open a route towards fully integrated and thus scalable quantum information processing.

Acknowledgement

The authors thank Silke Kuhn for fabricating the waveguide samples, and also Hanna Sala-

mon and Jakub Jasiński for the initial characterization of the ring resonator devices. Ł.D. acknowledges the financial support from the Alexander von Humboldt Foundation. S.-H. K. acknowledges the financial support from the National Research Foundation of Korea through the Korean Government Grant No. NRF-2019R1A2C4069587. We are furthermore grateful for the support by the State of Bavaria.

Supporting Information Available

The Supporting Information is available free of charge:
Methods; Simulation details; Waveguide modes; Waveguide transmission losses; Circular Bragg reflector, inverse taper out-couplers and mode converters details; Ring design optimization; Extraction efficiency estimation; Two-photon interference histogram fitting and visibility correction; Performance of other ring resonator devices.

References

(1) Santori, C.; Fattal, D.; Vucković, J.; Solomon, G. S.; Yamamoto, Y. Indistinguishable photons from a single-photon device. *Nature* **2002**, *419*, 594–7.

(2) Aharonovich, I.; Englund, D.; Toth, M. Solid-state single-photon emitters. *Nature Photonics* **2016**, *10*, 631–641.

(3) Senellart, P.; Solomon, G.; White, A. High-performance semiconductor quantum-dot single-photon sources. *Nature Nanotechnology* **2017**, *12*, 1026–1039.

(4) Somaschi, N. et al. Near-optimal single-photon sources in the solid state. *Nature Photonics* **2016**, *10*, 340–345.

(5) Unsleber, S.; He, Y.-M.; Maier, S.; Gerhardt, S.; Lu, C.-Y.; Pan, J.-W.; Kamp, M.; Schneider, C.; Höfling, S. Highly indistinguishable on-demand resonance fluorescence

photons from a deterministic quantum dot micropillar device with 75% extraction efficiency. *Optics express* **2016**, *24*, 8539–8546.

(6) Wang, H. et al. Towards optimal single-photon sources from polarized microcavities. *Nature Photonics* **2019**, *13*, 770–775.

(7) Pooley, M. A.; Ellis, D. J. P.; Patel, R. B.; Bennett, A. J.; Chan, K. H. A.; Farrer, I.; Ritchie, D. A.; Shields, A. J. Controlled-NOT gate operating with single photons. *Applied Physics Letters* **2012**, *100*, 211103.

(8) Gazzano, O.; Almeida, M. P.; Nowak, A. K.; Portalupi, S. L.; Lemaître, A.; Sagnes, I.; White, A. G.; Senellart, P. Entangling Quantum-Logic Gate Operated with an Ultrabright Semiconductor Single-Photon Source. *Physical Review Letters* **2013**, *110*, 250501.

(9) He, Y.-M.; He, Y.; Wei, Y.-J.; Wu, D.; Atatüre, M.; Schneider, C.; Höfling, S.; Kamp, M.; Lu, C.-Y.; Pan, J.-W. On-demand semiconductor single-photon source with near-unity indistinguishability. *Nature Nanotechnology* **2013**, *8*, 213–217.

(10) Delteil, A.; Sun, Z.; Gao, W.-b.; Togan, E.; Faelt, S.; Imamoglu, A. Generation of heralded entanglement between distant hole spins. *Nature Physics* **2015**, *12*, 218–223.

(11) Stockill, R.; Stanley, M. J.; Huthmacher, L.; Clarke, E.; Hugues, M.; Miller, A. J.; Matthiesen, C.; Le Gall, C.; Atatüre, M. Phase-Tuned Entangled State Generation between Distant Spin Qubits. *Physical Review Letters* **2017**, *119*, 010503.

(12) Nilsson, J.; Stevenson, R. M.; Chan, K. H. A.; Skiba-Szymanska, J.; Lucamarini, M.; Ward, M. B.; Bennett, A. J.; Salter, C. L.; Farrer, I.; Ritchie, D. A.; Shields, A. J. Quantum teleportation using a light-emitting diode. *Nature Photonics* **2013**, *7*, 311–315.

(13) Reindl, M.; Huber, D.; Schimpf, C.; da Silva, S. F. C.; Rota, M. B.; Huang, H.; Zwiller, V.; Jöns, K. D.; Rastelli, A.; Trotta, R. All-photonic quantum teleportation using on-demand solid-state quantum emitters. *Science Advances* **2018**, *4*, eaau1255.

(14) Wang, H. et al. Multi-photon boson-sampling machines beating early classical computers. *arXiv:1612.06956* **2019**,

(15) Flagg, E. B.; Muller, A.; Robertson, J. W.; Founta, S.; Deppe, D. G.; Xiao, M.; Ma, W.; Salamo, G. J.; Shih, C. K. Resonantly driven coherent oscillations in a solid-state quantum emitter. *Nature Physics* **2009**, *5*, 203–207.

(16) Ates, S.; Ulrich, S. M.; Reitzenstein, S.; Löffler, A.; Forchel, A.; Michler, P. Post-Selected Indistinguishable Photons from the Resonance Fluorescence of a Single Quantum Dot in a Microcavity. *Physical Review Letters* **2009**, *103*, 167402.

(17) Iles-Smith, J.; McCutcheon, D. P. S.; Nazir, A.; Mørk, J. Phonon scattering inhibits simultaneous near-unity efficiency and indistinguishability in semiconductor single-photon sources. *Nature Photonics* **2017**, *11*, 521–526.

(18) Dietrich, C. P.; Fiore, A.; Thompson, M. G.; Kamp, M.; Höfling, S. GaAs integrated quantum photonics: Towards compact and multi-functional quantum photonic integrated circuits. *Laser & Photonics Reviews* **2016**, *10*, 870.

(19) Hepp, S.; Jetter, M.; Portalupi, S. L.; Michler, P. Semiconductor Quantum Dots for Integrated Quantum Photonics. *Advanced Quantum Technologies* **2019**, *1900020*, 1900020.

(20) Jöns, K. D.; Rengstl, U.; Oster, M.; Hargart, F.; Heldmaier, M.; Bounouar, S.; Ulrich, S. M.; Jetter, M.; Michler, P. Monolithic on-chip integration of semiconductor waveguides, beamsplitters and single-photon sources. *Journal of Physics D: Applied Physics* **2015**, *48*, 085101.

(21) Enderlin, A.; Ota, Y.; Ohta, R.; Kumagai, N.; Ishida, S.; Iwamoto, S.; Arakawa, Y. High guided modecavity mode coupling for an efficient extraction of spontaneous emission of a single quantum dot embedded in a photonic crystal nanobeam cavity. *Physical Review B* **2012**, *86*, 075314.

(22) Schwagmann, A.; Kalliakos, S.; Farrer, I.; Griffiths, J. P.; Jones, G. A. C.; Ritchie, D. A.; Shields, A. J. On-chip single photon emission from an integrated semiconductor quantum dot into a photonic crystal waveguide. *Applied Physics Letters* **2011**, *99*, 261108.

(23) Arcari, M.; Söllner, I.; Javadi, A.; Lindskov Hansen, S.; Mahmoodian, S.; Liu, J.; Thyrrestrup, H.; Lee, E. H.; Song, J. D.; Stobbe, S.; Lodahl, P. Near-Unity Coupling Efficiency of a Quantum Emitter to a Photonic Crystal Waveguide. *Physical Review Letters* **2014**, *113*, 093603.

(24) Reithmaier, G.; Kaniber, M.; Flassig, F.; Lichtmannecker, S.; Müller, K.; Andrejew, A.; Vučković, J.; Gross, R.; Finley, J. J. On-Chip Generation, Routing, and Detection of Resonance Fluorescence. *Nano Letters* **2015**, *15*, 5208–5213.

(25) Davanco, M.; Liu, J.; Sapienza, L.; Zhang, C.-Z.; De Miranda Cardoso, J. V.; Verma, V.; Mirin, R.; Nam, S. W.; Liu, L.; Srinivasan, K. Heterogeneous integration for on-chip quantum photonic circuits with single quantum dot devices. *Nature Communications* **2017**, *8*, 889.

(26) Elshaari, A. W.; Zadeh, I. E.; Fognini, A.; Reimer, M. E.; Dalacu, D.; Poole, P. J.; Zwiller, V.; Jöns, K. D. On-chip single photon filtering and multiplexing in hybrid quantum photonic circuits. *Nature Communications* **2017**, *8*, 379.

(27) Kim, J.-H.; Aghaeimeibodi, S.; Richardson, C. J. K.; Leavitt, R. P.; Englund, D.; Waks, E. Hybrid Integration of Solid-State Quantum Emitters on a Silicon Photonic Chip. *Nano Letters* **2017**, *17*, 7394.

(28) Ellis, D. J. P.; Bennett, A. J.; Dangel, C.; Lee, J. P.; Griffiths, J. P.; Mitchell, T. A.; Paraiso, T.-K.; Spencer, P.; Ritchie, D. A.; Shields, A. J. Independent indistinguishable quantum light sources on a reconfigurable photonic integrated circuit. *Applied Physics Letters* **2018**, *112*, 211104.

(29) Midolo, L.; Hansen, S. L.; Zhang, W.; Papon, C.; Schott, R.; Ludwig, A.; Wieck, A. D.; Lodahl, P.; Stobbe, S. Electro-optic routing of photons from a single quantum dot in photonic integrated circuits. *Opt. Express* **2017**, *25*, 33514–33526.

(30) Wang, J. et al. Gallium arsenide (GaAs) quantum photonic waveguide circuits. *Optics Communications* **2014**, *327*, 49–55.

(31) Prtljaga, N.; Coles, R. J.; O'Hara, J.; Royall, B.; Clarke, E.; Fox, A. M.; Skolnick, M. S. Monolithic integration of a quantum emitter with a compact on-chip beam-splitter. *Applied Physics Letters* **2014**, *104*, 231107.

(32) Elshaari, A. W.; Büyüközer, E.; Zadeh, I. E.; Lettner, T.; Zhao, P.; Schöll, E.; Gyger, S.; Reimer, M. E.; Dalacu, D.; Poole, P. J.; Jöns, K. D.; Zwiller, V. Strain-Tunable Quantum Integrated Photonics. *Nano Letters* **2018**, *18*, 7969–7976.

(33) Aghaeimeibodi, S.; Kim, J.-H.; Lee, C.-M.; Buyukkaya, M. A.; Richardson, C.; Waks, E. Silicon photonic add-drop filter for quantum emitters. *Optics Express* **2019**, *27*, 16882.

(34) Kaniber, M.; Flassig, F.; Reithmaier, G.; Gross, R.; Finley, J. J. Integrated superconducting detectors on semiconductors for quantum optics applications. *Applied Physics B* **2016**, *122*, 115.

(35) Makhonin, M. N.; Dixon, J. E.; Coles, R. J.; Royall, B.; Luxmoore, I. J.; Clarke, E.; Hugues, M.; Skolnick, M. S.; Fox, A. M. Waveguide Coupled Resonance Fluorescence from On-Chip Quantum Emitter. *Nano Letters* **2014**, *14*, 6997–7002.

(36) Kalliakos, S.; Brody, Y.; Bennett, A. J.; Ellis, D. J. P.; Skiba-Szymanska, J.; Farrer, I.; Griffiths, J. P.; Ritchie, D. A.; Shields, A. J. Enhanced indistinguishability of in-plane single photons by resonance fluorescence on an integrated quantum dot. *Applied Physics Letters* **2016**, *109*, 151112.

(37) Schwartz, M.; Rengstl, U.; Herzog, T.; Paul, M.; Kettler, J.; Portalupi, S. L.; Jetter, M.; Michler, P. Generation, guiding and splitting of triggered single photons from a resonantly excited quantum dot in a photonic circuit. *Optics Express* **2016**, *24*, 3089–3094.

(38) Kiršansk, G. et al. Indistinguishable and efficient single photons from a quantum dot in a planar nanobeam waveguide. *Physical Review B* **2017**, *96*, 165306.

(39) Liu, F.; Brash, A. J.; O'Hara, J.; Martins, L. M. P. P.; Phillips, C. L.; Coles, R. J.; Royall, B.; Clarke, E.; Bentham, C.; Prtljaga, N.; Itskevich, I. E.; Wilson, L. R.; Skolnick, M. S.; Fox, A. M. High Purcell factor generation of indistinguishable on-chip single photons. *Nature Nanotechnology* **2018**, *13*, 835–840.

(40) Dusanowski, Ł.; Kwon, S.-h.; Schneider, C.; Höfling, S. Near-Unity Indistinguishability Single Photon Source for Large-Scale Integrated Quantum Optics. *Physical Review Letters* **2019**, *122*, 173602.

(41) Lund-Hansen, T.; Stobbe, S.; Julsgaard, B.; Thyrrestrup, H.; Sünner, T.; Kamp, M.; Forchel, A.; Lodahl, P. Experimental Realization of Highly Efficient Broadband Coupling of Single Quantum Dots to a Photonic Crystal Waveguide. *Physical Review Letters* **2008**, *101*, 113903.

(42) Stepanov, P.; Delga, A.; Zang, X.; Bleuse, J.; Dupuy, E.; Peinke, E.; Lalanne, P.; Gérard, J.-M.; Claudon, J. Quantum dot spontaneous emission control in a ridge waveguide. *Applied Physics Letters* **2015**, *106*, 041112.

(43) Fattah poor, S.; Hoang, T. B.; Midolo, L.; Dietrich, C. P.; Li, L. H.; Linfield, E. H.; Schouwenberg, J. F. P.; Xia, T.; Pagliano, F. M.; van Otten, F. W. M.; Fiore, A.

Efficient coupling of single photons to ridge-waveguide photonic integrated circuits. *Applied Physics Letters* **2013**, *102*, 131105.

(44) Schwartz, M.; Schmidt, E.; Rengstl, U.; Hornung, F.; Hepp, S.; Portalupi, S. L.; Llin, K.; Jetter, M.; Siegel, M.; Michler, P. Fully On-Chip Single-Photon Hanbury-Brown and Twiss Experiment on a Monolithic SemiconductorSuperconductor Platform. *Nano Letters* **2018**, *18*, 6892–6897.

(45) Reigue, A.; Iles-Smith, J.; Lux, F.; Monniello, L.; Bernard, M.; Margaillan, F.; Lemaitre, A.; Martinez, A.; McCutcheon, D. P.; Mørk, J.; Hostein, R.; Voliotis, V. Probing Electron-Phonon Interaction through Two-Photon Interference in Resonantly Driven Semiconductor Quantum Dots. *Physical Review Letters* **2017**, *118*, 233602.

(46) Hepp, S.; Bauer, S.; Hornung, F.; Schwartz, M.; Portalupi, S. L.; Jetter, M.; Michler, P. Bragg grating cavities embedded into nano-photonic waveguides for Purcell enhanced quantum dot emission. *Optics Express* **2018**, *26*, 30614.

(47) *Integrated Ring Resonators: The Compendium*; Springer Berlin Heidelberg: Berlin, Heidelberg, 2007; pp 3–40.

(48) Wen, Y. H.; Kuzucu, O.; Hou, T.; Lipson, M.; Gaeta, A. L. All-optical switching of a single resonance in silicon ring resonators. *Optics Letters* **2011**, *36*, 1413.

(49) Engin, E.; Bonneau, D.; Natarajan, C. M.; Clark, A. S.; Tanner, M. G.; Hadfield, R. H.; Dorenbos, S. N.; Zwiller, V.; Ohira, K.; Suzuki, N.; Yoshida, H.; Iizuka, N.; Ezaki, M.; O'Brien, J. L.; Thompson, M. G. Photon pair generation in a silicon micro-ring resonator with reverse bias enhancement. *Optics Express* **2013**, *21*, 27826.

(50) Faraon, A.; Barclay, P. E.; Santori, C.; Fu, K.-M. C.; Beausoleil, R. G. Resonant enhancement of the zero-phonon emission from a colour centre in a diamond cavity. *Nature Photonics* **2011**, *5*, 301–305.

(51) Kuan Pei Yap,; Delage, A.; Lapointe, J.; Lamontagne, B.; Schmid, J.; Waldron, P.; Syrett, B.; Janz, S. Correlation of Scattering Loss, Sidewall Roughness and Waveguide Width in Silicon-on-Insulator (SOI) Ridge Waveguides. *Journal of Lightwave Technology* **2009**, *27*, 3999–4008.

(52) Gerhardt, S.; Iles-Smith, J.; McCutcheon, D. P. S.; He, Y.-M.; Unsleber, S.; Betzold, S.; Gregersen, N.; Mørk, J.; Höfling, S.; Schneider, C. Intrinsic and environmental effects on the interference properties of a high-performance quantum dot single-photon source. *Physical Review B* **2018**, *97*, 195432.

(53) Rengstl, U.; Schwartz, M.; Herzog, T.; Hargart, F.; Paul, M.; Portalupi, S. L.; Jetter, M.; Michler, P. On-chip beamsplitter operation on single photons from quasi-resonantly excited quantum dots embedded in GaAs rib waveguides. *Applied Physics Letters* **2015**, *107*, 021101.

(54) Varnava, M.; Browne, D. E.; Rudolph, T. How Good Must Single Photon Sources and Detectors Be for Efficient Linear Optical Quantum Computation? *Physical Review Letters* **2008**, *100*, 060502.

(55) Fowler, A. G.; Stephens, A. M.; Groszkowski, P. High-threshold universal quantum computation on the surface code. *Physical Review A* **2009**, *80*, 052312.

Graphic for Table of Content only